

# Ab Initio Study of the Catalytic Reactivity of Titanosilsesquioxanes and Titanosiloxanes

Takako Kudo\*

Department of Fundamental Studies, Faculty of Engineering, Gunma University, Kiryu 376-8515, Japan

Mark S. Gordon\*

Department of Chemistry, Iowa State University, Ames, Iowa 50011-2030

Received: June 13, 2003; In Final Form: August 5, 2003

The catalytic reactivity of titanosilsesquioxanes and titanosiloxanes are investigated with ab initio electronic structure theory including electron correlation effects. The reactions examined are the oxidation of olefins and polymerization of ethylene. The titanium compounds are found to be promising effective catalysts for the oxidation reactions, with the catalytic activity increasing with the number of Ti-containing substituents. Ring and cage structures also enhance the catalytic ability of these compounds, whereas the addition of Si-containing substituents has the opposite effect. The same Ti compounds are predicted to be less effective as catalysts for ethylene polymerization.

## Introduction

Titanium compounds are well-known as effective catalysts, especially for various olefin oxidation<sup>1</sup> and polymerization reactions.<sup>2</sup> Recently, the results of some experimental studies suggested that Ti-modified silicates (titanosilicates) and amorphous silica-supported titanium exhibit efficient catalytic activity for olefin oxidation by H<sub>2</sub>O<sub>2</sub> or ROOH.<sup>3</sup> Theoretical calculations have also been performed for these reactions, primarily with density functional theory (DFT).<sup>4</sup> Using a variety of models, the predicted activation energies for the oxidation of olefins are in the range of 10–17 kcal/mol.

Silicates and silica contain Si–O–Si linkages that are also the backbone of another class of compounds, polyhedral oligomeric silsesquioxanes (POSS). The mechanisms by which POSS are formed have been of interest to the authors for many years.<sup>5,6</sup> Recently, the structure and properties of several POSS titanium analogues (Ti–POSS) and Si/Ti-mixed POSS have been analyzed, with the ultimate goal of designing new functional POSS species.<sup>7</sup> Therefore, a logical extension of these studies is an investigation of the reactivity of the titanium compounds. In the present work, the catalytic ability of Ti–POSS species is investigated using ab initio electronic structure methods.

The catalytic reactions presented here are the oxidation of ethylene and butadiene, and the polymerization of ethylene. Of primary interest is the relation between the molecular structure and reactivity. An additional focus is on the effect of the number of titanium atoms and silicon atoms in the Si/Ti-mixed siloxanes and POSS on their catalytic abilities.

## Computational Methods

The geometries of all molecules of interest have been fully optimized at the restricted Hartree–Fock (RHF) and the B3LYP hybrid density functional levels of theory<sup>8</sup> using the 6-31G(d) basis set.<sup>9</sup> In addition, the geometries of smaller and some key systems were refined using second-order perturbation theory

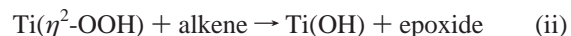
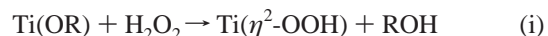
(MP2)<sup>10</sup> and the triple- $\zeta$  plus polarization function basis sets, TZVP, developed by Wachters.<sup>11</sup> For Ti, the Wachters Gaussian basis set (14s,11p,6d) contracted to [10s,8p,3d] with some modification was used.<sup>12,13</sup> A contracted Gaussian basis set (13s,9p)/[6s,5p] augmented with a set of *d*-type functions ( $\alpha_d = 0.388$ ) was used for Si, while a contracted Gaussian basis set (11s,6p)/[5s,3p] augmented with a set of *d*-type functions was employed for C ( $\alpha_d = 0.72$ ) and O ( $\alpha_d = 1.28$ ), and (5s)/[3s] with a set of *p*-type function ( $\alpha_p = 1.0$ ) was used for H. All compounds were characterized as minima or transition states by calculating and diagonalizing the Hessian matrix of energy second derivatives. Furthermore, IRC calculations were performed to verify the connection between the minima and transition structures for some key reactions, as specified in the following discussion. Single-point MP2 energy calculations have been performed to obtain more reliable energetics. All calculations were performed with the GAMESS<sup>12</sup> and Gaussian electronic structure codes.<sup>14</sup>

## Results and Discussion

**A. Oxidation of Ethylene.** The mechanism of oxidation of olefins by titanium catalysts has been proposed as the following two-step reaction:

(i) The formation of an oxygen-donating complex, Ti( $\eta^2$ -OOH), from the titanium compound and H<sub>2</sub>O<sub>2</sub>, and

(ii) An oxygen transfer from the complex to the olefin. This mechanism is based on a proposal by Sharpless for the Ti<sup>IV</sup>-catalyzed epoxidation using alkyl hydroperoxides.<sup>15</sup>



There has been some discussion regarding the most likely active oxygen-donating intermediate complex generated in the first step,<sup>1a</sup> but Ti( $\eta^2$ -OOR) seems to be the favored candidate. Once this intermediate is formed, the alkene accepts an oxygen atom from the complex, and an epoxide is formed in the second step as the final product.

\* Corresponding authors.

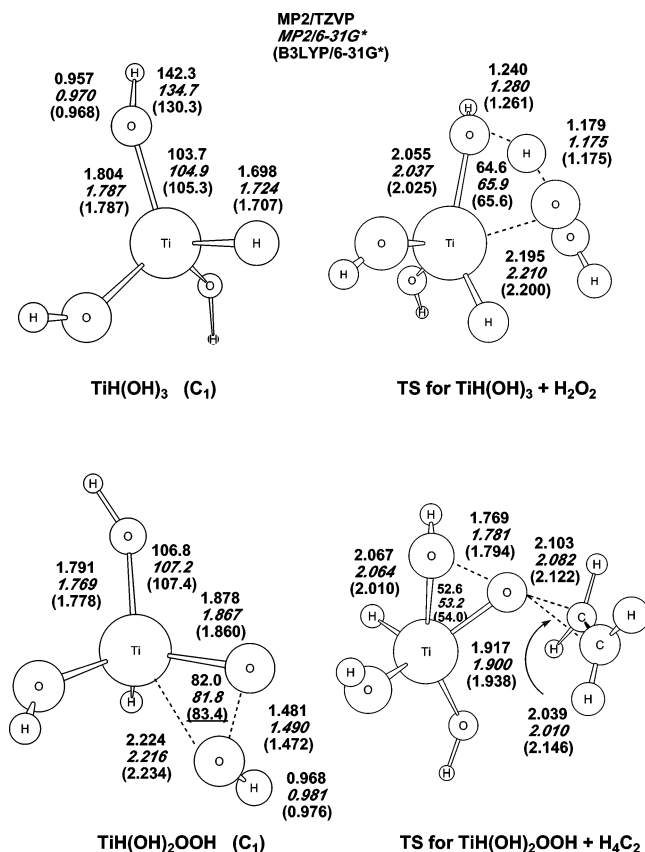
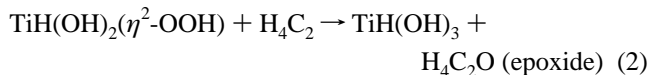


**Figure 1.** Optimized structures of some stationary points on the potential energy surface of the oxidation of ethene with  $\text{TiH}(\text{OH})_3$  and  $\text{H}_2\text{O}_2$  in angstroms and degrees.

To analyze the catalytic mechanism, the first step in the work presented here was to examine the simple model compound trihydroxytitanane ( $\text{TiH}(\text{OH})_3$ ), as the titanium catalyst, to scan the potential energy surface in detail. The reaction is represented by the following reactions:



The optimized geometries for the most important stationary points are displayed in Figure 1, and the potential energy surfaces for the first and second steps of the reaction mechanism are shown in Figures 2 and 3, respectively. As the figures show, the first step in the reaction proceeds via two intermediate complexes and one transition state that connects the two intermediates. In the second step, one intermediate complex has been located, as well as the transition structure that connects the complex and products, as confirmed by the IRC calculation. In the complex in the second step, one OH bonds to the ethylene CC  $\pi$ -bond. Another complex has been located in which Ti bonds directly to the ethylene CC  $\pi$ -bond. However, this second complex is slightly higher in energy than the one shown in Figure 3, and it is not connected to the transition state.

In reaction 1, the two reactant molecules form the first intermediate complex. Then, one hydrogen atom is transferred from  $\text{H}_2\text{O}_2$  to one titanol OH group in the transition structure. Finally, the active oxygen-donating complex,  $\text{TiH}(\text{OH})_2(\eta^2\text{-OOH})$  and  $\text{H}_2\text{O}$  are formed via the second intermediate complex. For  $\text{TiH}(\text{OH})_2(\eta^2\text{-OOH})$ , the two Ti–O distances to the OOH

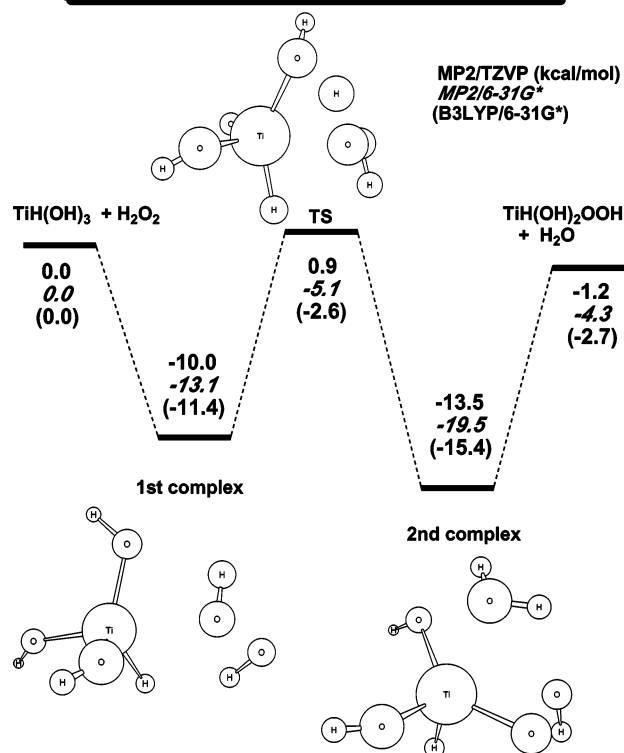


**Figure 2.** The potential energy profile for the first step in the oxidation of ethene with  $\text{TiH}(\text{OH})_3$  and  $\text{H}_2\text{O}_2$  at three levels of theory.

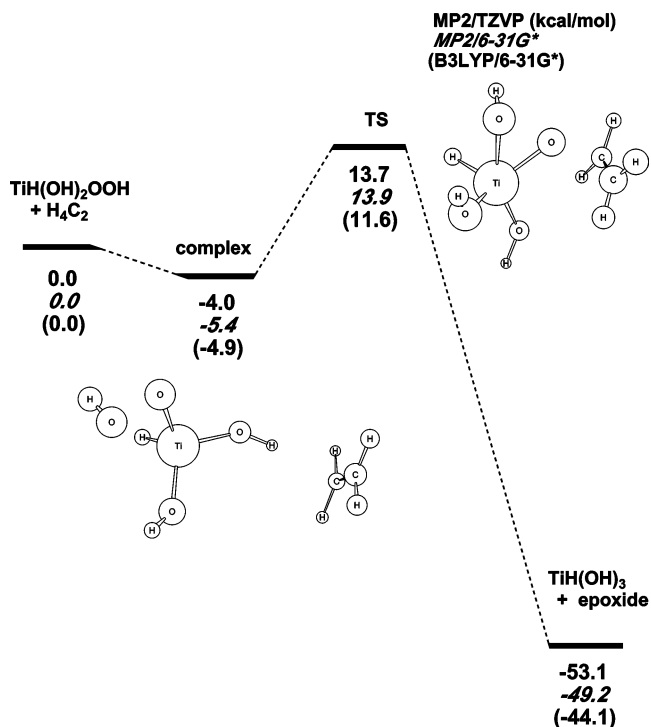
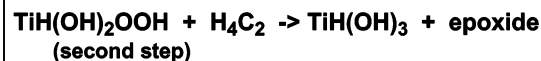


**Figure 3.** The potential energy profile for the second step in the oxidation of ethene with  $\text{TiH}(\text{OH})_3$  and  $\text{H}_2\text{O}_2$  at three levels of theory.

group are rather different (See Figure 1), so this is not strictly an  $\eta^2$  structure. However, the difference decreases in the

**TABLE 1: Relative Energies (kcal/mol) for the Two Steps in the Oxidation of Ethylene with TiH(OH)<sub>3</sub> and H<sub>2</sub>O<sub>2</sub> at Various Levels of Theory**

	TiH(OH) <sub>3</sub> + H <sub>2</sub> O <sub>2</sub> → TiH(OH) <sub>2</sub> OOH + H <sub>2</sub> O (Step 1)					TiH(OH) <sub>2</sub> OOH + H <sub>2</sub> C <sub>2</sub> → TiH(OH) <sub>3</sub> +epoxide (Step 2)			
	R	CM1	TS	CM2	P	R	CM	TS	P
B3LYP/6-31G*	0.0	-11.4	-2.6	-15.4	-2.7	0.0	-4.9	11.8	-45.3
MP2/6-31G* <sup>a</sup>	0.0	-13.0	-4.7	-19.2	-4.2	0.0	-6.0	15.2	-49.3
MP2/6-31G*	0.0	-13.1	-5.1	-19.5	-4.3	0.0	-5.4	13.9	-49.2
MP2/TZVP	0.0	-10.0	0.9	-13.5	-1.2	0.0	-4.0	13.7	-53.1

<sup>a</sup> MP2/6-31G\* energy based on the B3LYP/6-31G\* optimized geometry.

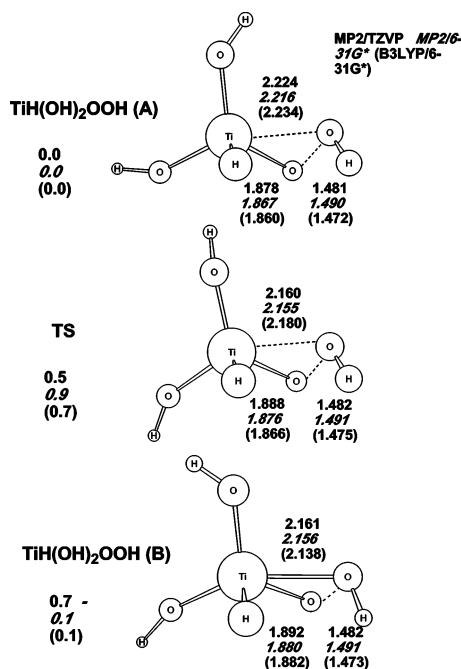


**Figure 4.** Two types of isomer of TiH(OH)<sub>2</sub>OOH and the transition state structure connecting them in angstroms and degrees with the relative energies in kcal/mol.

transition state. The structure of the  $\eta^2$ -OOH species is discussed in more detail below.

For step 1 the energies of the transition state and the reactants are nearly the same, suggesting that this first step in the reaction mechanism has essentially no barrier. On the other hand, the energy barrier for the oxidation of ethylene (second step) is about 12–13 kcal/mol. After the formation of the intermediate complex, the O atom that is closer to Ti is passed to ethylene at the transition state. Note that this reaction is highly exothermic, with a reaction energy of ~50 kcal/mol. The energies of all stationary points on the potential energy surfaces relative to the reactants are given in Table 1. The single-point MP2 calculations at the B3LYP/6-31G\* geometry give relative energies very similar to those obtained from the MP2/6-31G\* optimization. Furthermore, the B3LYP geometry is similar to the MP2 geometry (Figure 1). Therefore, the primary level of theory used in the results reported below is MP2/6-31G\*//B3LYP/6-31G\*.

Prior to the discussion of the oxidation of various titanium compounds, it is important to consider a feature of the TiH(OH)<sub>2</sub>( $\eta^2$ -OOH) geometry. This molecule has two isomers, denoted A and B in Figure 4, with very similar geometries. The largest differences between these two isomers are the Ti–O distances. In isomer B, the Ti–O(H) distance has decreased by ~0.06 Å, relative to that in A, while the Ti–O(O) distance has increased slightly. Consequently, these two distances differ by only 0.27 Å in B, as compared with 0.35 Å in A. So, isomer B

**TABLE 2: The Energy (kcal/mol) of Isomer B Isomer Relative to Isomer A Isomer of [Ti]RR'OOH at Three Levels of Theory**

titanoxanes	energy (kcal/mol)		
	B3LYP/6-31G*	MP2/6-31G*	MP2/TZVP//B3LYP/6-31G*
TiH(OH) <sub>2</sub> OOH	0.1 (-0.1) <sup>a</sup>	0.01	0.7
TiH(OSiH <sub>3</sub> )(OTiH <sub>3</sub> )OOH (D <sub>3</sub> ring)	-8.1	-12.7	
Ti <sub>3</sub> O <sub>3</sub> H <sub>5</sub> OOH (T <sub>4</sub> cage)	-6.8	-9.5	
Ti <sub>4</sub> O <sub>6</sub> H <sub>3</sub> OOH	-6.7	-9.2	

<sup>a</sup> MP2/6-31G\*//MP2/6-31G\*.

**TABLE 3: Energy Barriers (kcal/mol) for the Second Step in the Oxidation of Ethylene with Various Titanoxane Compounds, at the B3LYP/6-31G\* Geometries**

titanoxanes	energy barriers (kcal/mol)	
	B3LYP/6-31G*	MP2/6-31G*
TiH(OH) <sub>2</sub> OOH	11.6	15.2
TiH(OSiH <sub>3</sub> ) <sub>2</sub> OOH	11.8	14.8
TiH(OSiH <sub>3</sub> )(OTiH <sub>3</sub> )OOH	8.4	10.9
TiH(OTiH <sub>3</sub> ) <sub>2</sub> OOH	6.2	8.4
Ti(OSiH <sub>3</sub> ) <sub>3</sub> OOH	14.5	15.8
Ti(OSiH <sub>3</sub> )(OTiH <sub>3</sub> ) <sub>2</sub> OOH	11.6	12.7
Ti(OTiH <sub>3</sub> ) <sub>3</sub> OOH	11.2	12.3
(D <sub>3</sub> ring)		
Ti <sub>3</sub> O <sub>3</sub> H <sub>5</sub> OOH	6.9	9.5
(D <sub>4</sub> ring)		
Ti <sub>2</sub> Si <sub>2</sub> O <sub>4</sub> H <sub>7</sub> OOH(C <sub>2v</sub> )	6.2	5.1
Ti <sub>2</sub> Si <sub>2</sub> O <sub>4</sub> H <sub>7</sub> OOH(D <sub>2h</sub> )	10.2	13.7
Ti <sub>4</sub> O <sub>4</sub> H <sub>7</sub> OOH	4.2	3.3
(T <sub>4</sub> and T <sub>8</sub> cage)		
Ti <sub>4</sub> O <sub>6</sub> H <sub>3</sub> OOH	8.1	10.3
TiSi <sub>7</sub> O <sub>12</sub> H <sub>7</sub> OOH	12.3	14.5
Ti <sub>2</sub> Si <sub>6</sub> O <sub>12</sub> H <sub>7</sub> OOH	10.5	12.5
Ti <sub>8</sub> O <sub>12</sub> H <sub>7</sub> OOH	9.6	10.8

corresponds more closely to the designation  $\eta^2$ . The transition state that connects the two isomers (verified by IRC calculations) is also shown in Figure 4. The corresponding energy barrier is negligible in the mono titanium compound considered here. However, the stability of the “five-coordinated” isomer B increases as the number of titanium atoms increases, as is shown in Table 2. Therefore, the complex is expected to have a five-coordinated structure corresponding to B in most cases considered here.

Since the calculations on the titanol system (Figures 2 and 3) suggest that the oxygen-donating reaction in which an O is transferred from TiH(OH)<sub>2</sub>( $\eta^2$ -OOH) to ethylene is the rate-determining step, the energy barrier for this second step has been determined for various titanium compounds as summarized in Table 3. The B3LYP/6-31G\* optimized transition structures of some of these compounds are displayed in Figure 5. The

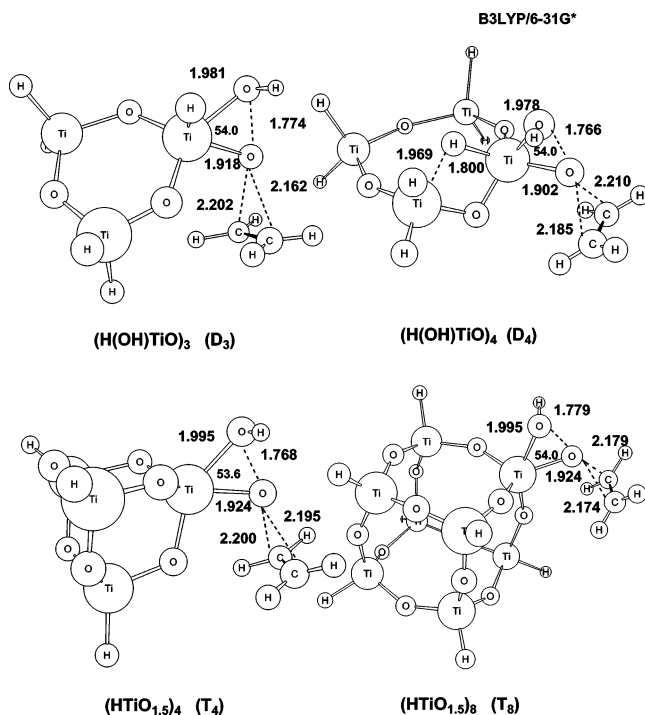
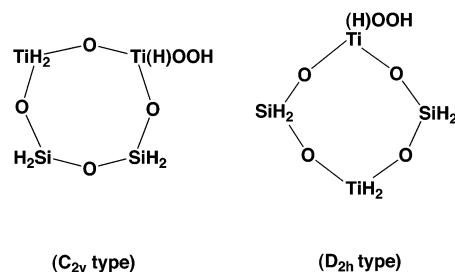


**Figure 5.** Transition structures for the second step in the oxidation of ethene with some titanoxanes in angstroms and degrees.

geometry of the reaction center seems to be independent of the remaining ligands bonded to the titanium atom. Note that the D<sub>4</sub> ring is markedly deformed such that the hydrogen attached to the reacting Ti is likely bridged to an adjacent Ti. As the figure shows, the distance between the hydrogen and the adjacent Ti is 1.969 Å, ~0.17 Å longer than a typical Ti–H bond distance. The electron density accumulated in this region is 0.103 e<sup>-</sup>. This is only slightly smaller than the 0.196 e<sup>-</sup> in the original Ti(reacting)–H bond. As a result, there appear to be two five-coordinated titanium atoms in the transition structure. Interestingly, the ring and cage structures are essentially unaffected in the other transition states.

In general (Table 3), B3LYP and MP2 predict the same trends, with B3LYP usually predicting somewhat smaller barrier heights. For the acyclic compounds, the energy barrier decreases as the number of Ti atoms in the molecule increases. The reaction seems to be more difficult if one hydrogen is replaced by OR (R=SiH<sub>3</sub> or TiH<sub>3</sub>), as in the case of TiH(OSiH<sub>3</sub>)<sub>2</sub>OOH and Ti(OSiH<sub>3</sub>)<sub>3</sub>OOH, for example. For given substituents, the reaction of the ring compounds is found to take place relatively easily. The energy barrier for the D<sub>4</sub> system OOH (Ti<sub>4</sub>O<sub>4</sub>H<sub>7</sub>OOH) is the smallest in Table 3. The hydrogen bridges in these rings may be the stabilizing factor. The 1,2- (C<sub>2v</sub> type) vs 1,3- (D<sub>2h</sub> type) Si substitution has a significant affect on the barrier, since the barrier for C<sub>2v</sub> Ti<sub>2</sub>Si<sub>2</sub>O<sub>4</sub>H<sub>7</sub>OOH is much lower than that for the D<sub>2h</sub> type isomer (See Scheme 1). It was previously shown<sup>5</sup> that in Ti<sub>2</sub>Si<sub>2</sub>O<sub>4</sub>H<sub>8</sub>, the D<sub>2h</sub> structure with alternating Ti and Si is lower in energy than the C<sub>2v</sub> isomer. This stability of the D<sub>2h</sub> arrangement may lead to the higher barrier. The energy barriers for the cage structures (e.g., T<sub>4</sub> and T<sub>8</sub>) are intermediate between those of the linear and ring forms. Some experimental studies have suggested that a silsesquioxane with the T<sub>8</sub> structure (TiSi<sub>7</sub>O<sub>12</sub>H<sub>7</sub>OOH) or the corresponding dimer is an active catalyst for the epoxidation of alkenes.<sup>16</sup> In addition, one Ti-substituted POSS compound with a T<sub>8</sub> structure is regarded as the model for Ti catalysts immobilized on silica surfaces.<sup>17</sup> For all of the compounds considered here, it appears

## SCHEME 1



that Ti substitution tends to enhance the reaction, while Si substitution has the reverse effect.

Figure 6 shows the potential energy surface for the ethylene oxidation by the most effective catalyst, D<sub>4</sub>OOH (Ti<sub>4</sub>O<sub>4</sub>H<sub>7</sub>OOH). Each transition state has been connected to the corresponding minima by IRC calculations. The transition state for the second step lies lower in energy than reactants, and the energy barrier for the first step is very low. Therefore, this reaction is expected to take place very easily, suggesting that D<sub>4</sub>OOH should be an effective catalyst.

**B. Oxidation of Butadiene.** Next, consider butadiene, the smallest conjugated hydrocarbon. One goal of the present study is to investigate the effect of multiple titanium or silicon atoms on the reaction, and ethylene is too small to interact with several Ti or Si atoms in addition to the reaction center. Table 4 presents the energy barrier for the second step in the oxidation of butadiene by several Ti compounds. In all cases, the energy barrier is lower than that of ethylene. One explanation might be that as butadiene has a higher HOMO and lower LUMO than the corresponding molecular orbitals of ethylene, the interaction with Ti compounds will be larger than that in ethylene. In particular, the interaction between the olefin HOMO ( $\pi^*_{C=C}$ ) and the Ti LUMO ( $\sigma^*_{Ti-H}$ )<sup>7</sup> is important for this reaction. The results shown in Table 4 suggest that the oxidation of butadiene catalyzed by the ring or cage compounds and even some linear Ti compounds, such as TiH(OTiH<sub>3</sub>)<sub>2</sub>OOH, should proceed rapidly at room temperature.

Next, consider the effect of the position of the butadiene double bond that is not in the reaction center. Figure 7 shows two alternative transition structures for the oxidation of butadiene in the presence of TiH(OTiH<sub>3</sub>)(OSiH<sub>3</sub>)OOH. In Type I, the nonreacting double bond is close to the OTiH<sub>3</sub> group, while in Type II, the nonreacting double bond is close to the OSiH<sub>3</sub> group. The geometry of the reaction center in these two transition structures is similar, but the difference in the MP2/6-31G\* energy barrier is quite large – 6.4 kcal/mol for Type I and 15.5 kcal/mol for Type II. It appears that the proximity of the conjugated system to the OTiH<sub>3</sub> group is preferred for the reasons suggested in the previous paragraph. In contrast, the proximity of the OSiH<sub>3</sub> group is apparently unfavorable.

**C. Polymerization of Ethene.** Polymerization of olefins is another reaction that is catalyzed by Ti catalysts. Recently, for example, there have been experimental reports regarding the catalytic activity of some disilylated titanium silsesquioxane derivatives.<sup>18</sup> Of course, the most well-known Ti-catalyzed reaction is the Ziegler–Natta reaction. Also, several theoretical studies based on the Cossee model have been published.<sup>4</sup> The Cossee model<sup>19</sup> involves (i) olefin coordination to a vacant site of a Ti atom in a Ti-alkyl compound, and (ii) olefin insertion into the Ti–C bond through a four-centered transition state. In the present work, this mechanism has been investigated for the titanoxane and titanium–siloxane compounds of interest.

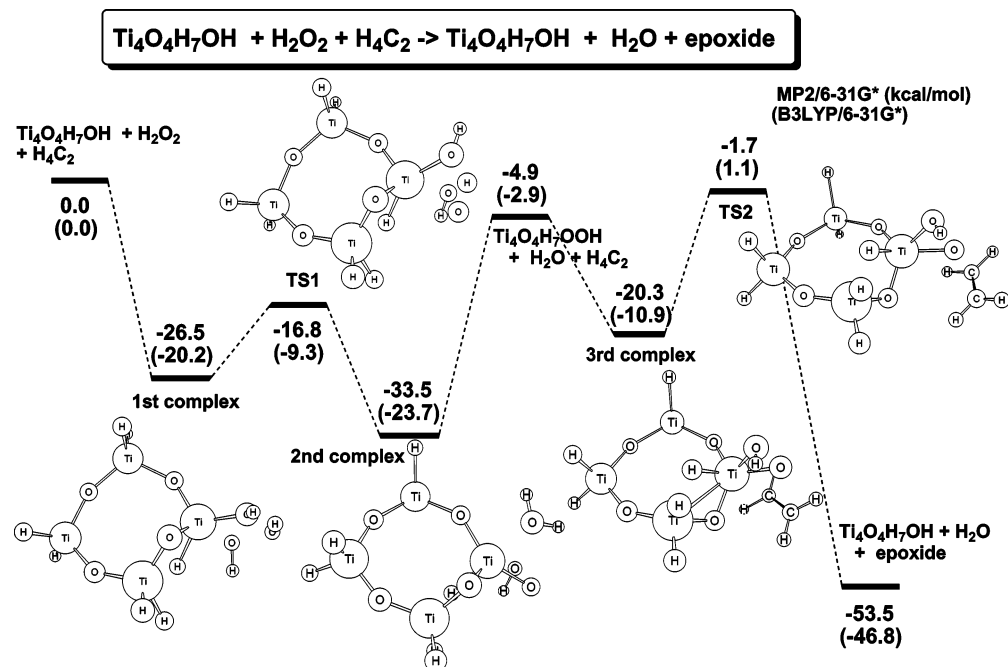
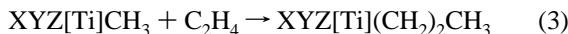


Figure 6. The potential energy profile for the oxidation of ethene with  $\text{Ti}_4\text{O}_4\text{H}_7\text{OH}$  and  $\text{H}_2\text{O}_2$ .

TABLE 4: Energy Barriers (kcal/mol) for the Second Step in the Oxidation of butadiene with Various Titanoxane Compounds, at B3LYP Geometries

titanoxanes	energy barriers (kcal/mol)	
	B3LYP/6-31G*	MP2/6-31G*
$\text{TiH}(\text{OH})_2\text{OOH}$	9.8	11.5
$\text{TiH}(\text{OSiH}_3)_2\text{OOH}$	11.2	12.6
$\text{TiH}(\text{OSiH}_3)(\text{OTiH}_3)\text{OOH}$ (I)	5.7	6.4
$\text{TiH}(\text{OSiH}_3)(\text{OTiH}_3)\text{OOH}$ (II)	11.7	15.5
$\text{TiH}(\text{OTiH}_3)_2\text{OOH}$	4.1	4.4
(D <sub>3</sub> ring)		
$\text{Ti}_3\text{O}_3\text{H}_3\text{OOH}$	4.8	4.7
(D <sub>4</sub> ring)		
$\text{Ti}_4\text{O}_5\text{H}_7\text{OOH}$	2.4	-0.02
(T <sub>4</sub> cage)		
$\text{Ti}_4\text{O}_6\text{H}_3\text{OOH}$	6.9	7.4

The catalysts employed here are methyl-substituted Ti compounds in the present work, and the reaction follows eq 3.



where X, Y, and Z are substituents on Ti.

First, consider the reaction of  $\text{Ti}(\text{OH})_3\text{CH}_3$ , the methyl-substituted analogue of  $\text{Ti}(\text{OH})_3\text{H}$ . A schematic of the MP2/6-31G\*  $\text{Ti}(\text{OH})_3\text{CH}_3 + \text{C}_2\text{H}_4$  potential energy surface is displayed in Figure 8. Also presented in this figure are the complex, the transition structure for insertion, and two structures along the IRC connecting the complex and the transition structure. The B3LYP/6-31G\* optimized geometries for the stationary points on the potential energy surface are shown in Figure 9. In the complex, ethylene coordinates with the hydrogen of one OH group of  $\text{Ti}(\text{OH})_3\text{CH}_3$ , rather than with the Ti atom. Then, the ethylene moves to the expected four-centered transition structure. However, as shown in Figure 8, there is a sizable (>20 kcal/mol) MP2 energy barrier, suggesting that  $\text{Ti}(\text{OH})_3\text{CH}_3$  is not an effective catalyst. The energy profile of this system is similar to that of  $\text{TiCH}_3\text{Cl}_3$  reported by Sakai for the case in which the cocatalyst  $\text{AlH}_2\text{Cl}$  is not present.<sup>20</sup>

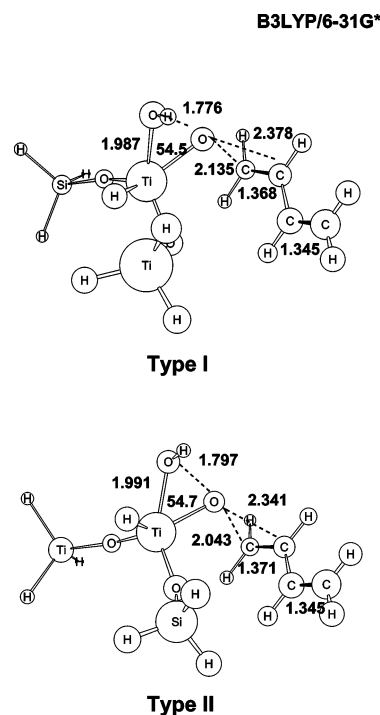
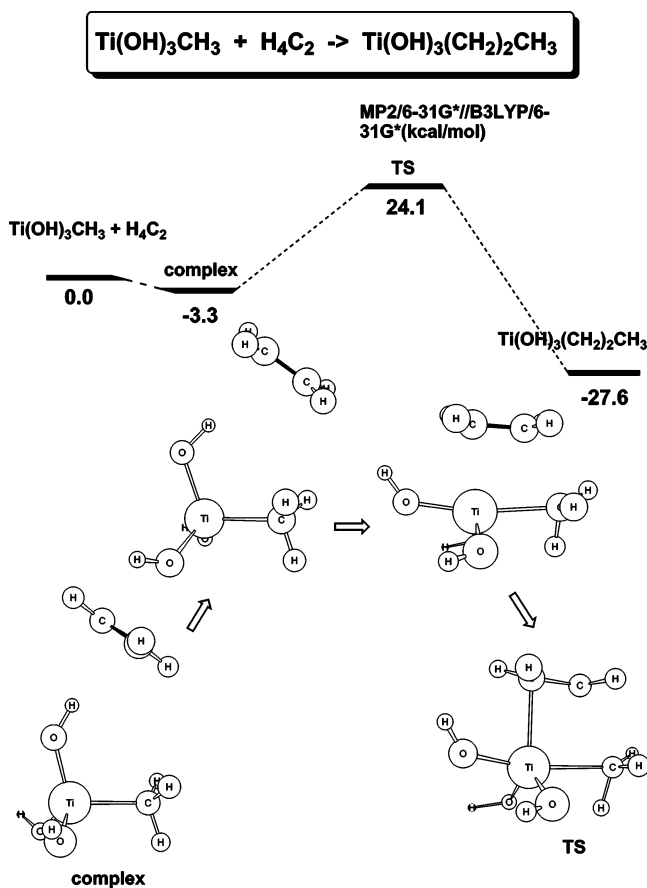


Figure 7. Two types of transition structures for the second step in the oxidation of butadiene with  $\text{TiH}(\text{OSiH}_3)(\text{OTiH}_3)\text{OH}$  and  $\text{H}_2\text{O}_2$  in angstroms and degrees.

The energy barriers for the same reaction using the other Ti compounds are collected in Table 5. For the acyclic compounds, substituting  $\text{OSiH}_3$  groups for OH groups has essentially no effect on the predicted barrier height. However,  $\text{OTiH}_3$  substitution dramatically reduces the barrier. One and two  $\text{OTiH}_3$  groups reduce the barrier to 15.8 and ~13 kcal/mol, respectively. In general, the energy barriers for the ring or cage compounds are predicted to be lower than those for the acyclic compounds. The T<sub>4</sub> compounds have slightly smaller energy barriers than the cyclic species, but these barriers are all greater than 10 kcal/mol. The B3LYP/6-31G\* transition structures for selected systems are shown in Figure 10. As the figure shows, the four-



**Figure 8.** The potential energy surface of the insertion reaction of ethene into  $\text{Ti(OH)}_3\text{CH}_3$  and the change of the molecular structures along the IRC connecting the complex with transition structure.

membered transition structures seem to bring about larger van der Waals repulsion compared to the oxidation reaction. Therefore, the present result suggests that, contrary to the oxidation reactions, the rate of polymerization of ethylene is not so enhanced by the presence of these titanium oxide compounds.

### Concluding Remarks

The ability of Ti-POSS, Ti/Si-mixed POSS, and other titanium oxide compounds to catalyze the oxidation and polymerization of olefins was investigated. Of particular interest is the relation between molecular structure and catalytic ability. The effect of the number of Ti atoms and the presence of Si atoms has also been considered.

For the oxidation of olefins (ethylene and butadiene), it is found that the second step — an oxygen transfer from Ti compounds to the olefin — is the rate-determining step. As the number of Ti atoms in the catalyst increases, the reaction takes place more easily. In contrast, Si atoms tend to increase the barrier. The energy barriers in the oxidation of ethylene decrease in the order, acyclic > cage > ring, and  $D_4$  has the smallest barrier. Butadiene exhibits higher reactivity than ethylene, possibly because of a higher energy HOMO in butadiene. Furthermore, it appears that having the conjugated system in close proximity to the Ti, rather than to Si, enhances the reaction.

For the polymerization of ethylene, the most effective catalyst appears to be the  $T_4$  cage species although the barrier is still greater than 10 kcal/mol. In general, the ring and cage structures seem to be more effective catalysts than the acyclic ones, but with significant (> 10 kcal/mol) barriers. So, the Ti compounds

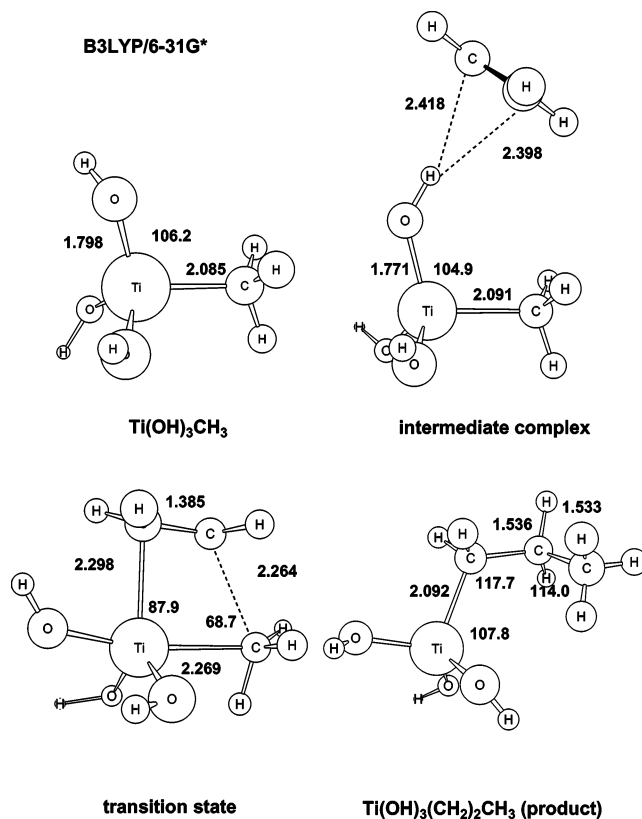


**Figure 9.** Optimized structures of the stationary points on the potential energy surface of the insertion reaction of ethene into  $\text{Ti(OH)}_3\text{CH}_3$  in angstroms and degrees.

**TABLE 5: Energy Barriers (kcal/mol) at the B3LYP Geometries for the Insertion of Ethylene into the Ti-CH<sub>3</sub> Bond of Various Titanoxane Compounds**

titanoxanes	energy barriers (kcal/mol)	
	B3LYP/6-31G*	MP2/6-31G*
$\text{Ti(OH)}_3\text{CH}_3$	26.1	24.1
$\text{TiOH(OSiH}_3)_2\text{CH}_3$	27.4	24.5
$\text{TiOH(OSiH}_3)(\text{OTiH}_3)\text{CH}_3$	22.1	15.8
$\text{TiOH(OTiH}_3)_2\text{CH}_3$	19.4	13.6 (13.0) <sup>a</sup>
(D <sub>3</sub> ring)		
$\text{Ti}_3\text{O}_3\text{H}_5\text{CH}_3$	20.9	15.9
(D <sub>4</sub> ring)		
$\text{Ti}_4\text{O}_3\text{H}_7\text{CH}_3$	20.2	13.2
(T <sub>4</sub> cage)		
$\text{Ti}_4\text{O}_6\text{H}_5\text{CH}_3$	18.1	12.0
(T <sub>8</sub> cage)		
$\text{Ti}_8\text{O}_{12}\text{H}_7\text{CH}_3$	21.4	14.4

<sup>a</sup> The MP2/6-31G\*//MP2/6-31G\* value.

studied in the present work are not expected to be desirable candidates for the catalysis of the polymerization of ethylene within the framework of the current mechanism.

Finally, Ti-POSS and Ti/Si-mixed POSS are expected to be effective catalysts for the oxidation of olefins. The ring structures are also good candidates, since they are even more active than the cage structures. A possibility not considered here is having the reaction occur *in the cage*. This intriguing possibility will be the subject of a future report.

**Acknowledgment.** This work has been supported by a Grant-in-Aid on Priority-Area Research: Material Design and Reaction Control by Molecular Physical Chemistry (11166212)-(T.K.) and the Air Force Office of Scientific Research (M.S.G.).

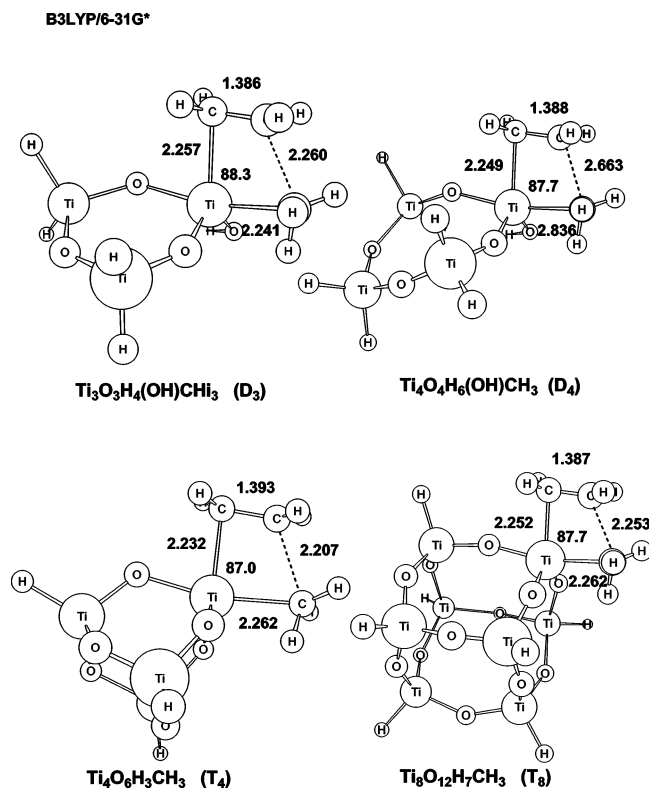


**Figure 10.** Transition structures for the insertion of ethene into the Ti-CH<sub>3</sub> bond of some titanoxanes in angstroms and degrees.

Computer time has been made available via a Grand Challenge grant from the DOD High Performance Computing Modernization Office on the T3E computers at ERDC and AHPARC and a grant from the Computer Center of the Institute for Molecular Science.

## References and Notes

- (1) (a) Murugavel, R.; Roesky, H. W. *Angew. Chem., Int. Ed. Engl.* **1997**, *36*, 477. (b) Sheldon, R. A.; Wallau, M.; Arends, I. W. C. E.; Schuchardt, U. *Acc. Chem. Res.* **1998**, *31*, 485. (c) Dusi, M.; Mallat, T.; Baiker, A. *Catal. Rev. Sci. Eng.* **2000**, *42*, 213.
- (2) (a) Ziegler, K.; Holzkamp, E.; Breil, H.; Martin, H. *Angew. Chem.* **1955**, *67*, 541. (b) Natta, T. *Macromol. Chem.* **1955**, *16*, 213. (c) Clawson, L.; Soto, J.; Buchwald, S. L.; Steigerwald, M. L.; Grubbs, R. H. *J. Am. Chem. Soc.* **1985**, *107*, 3377. (d) Erisch, J. J.; Piotrowski, A. M.; Brownstein, S. K.; Gabe, E. J.; Lee, F. L. *J. Am. Chem. Soc.* **1985**, *107*, 7219.
- (3) (a) Crocker, M.; Herold, R. H. M.; Orpen, A. G.; Overgaard, M. T. *A. J. Chem. Soc., Dalton Trans.* **1999**, 3791. (b) Thomas, J. M.; Sankar, G.; Klunduk, M. C.; Attfield, M. P.; Maschmeyer, T.; Johnson, B. F. G.; Bell, R. G. *J. Phys. Chem. B* **1999**, *103*, 8809. (c) Capel-Sanchez, M. C.; Campos-Martin, J. M.; Fierro, J. L. G.; de Frutos, M. P.; Padiella Polo, A. *Chem. Commun.* **2000**, 855. (d) Fraile, J. M.; Garcia, J. I.; Mayoral, J. A.; Vispe, E.; Brown, D. R.; Naderi, M. *Chem. Commun.* **2000**, 1510. (e) Murata, K.; Kiyozumi, Y. *Chem. Commun.* **2001**, 1356.
- (4) (a) Wu, Y.-D.; Lai, D. K. W. *J. Org. Chem.* **1995**, *60*, 673. (b) Tantanak, D.; Vincent, M. A.; Hillier, I. H. *Chem. Commun.* **1998**, 1031.
- (c) Sinclair, P. E.; Catlow, R. A. *J. Phys. Chem. B* **1999**, *103*, 1084.
- (5) For reviews, see for example, (a) Voronkov, M. G.; Lavrent'yev, V. L. *Top. Curr. Chem.* **1982**, *102*, 199. (b) Feher, F. J.; Newman, D. A.; Walzer, J. F. *J. Am. Chem. Soc.* **1989**, *1111*, 1741. (c) Baney, R. H.; Itoh, M.; Sakakibara, A.; Suzuki, T. *Chem. Rev.* **1995**, *95*, 1409. (d) Feher, F. J.; Budzichowski, T. A. *Polyhedron* **1995**, *14*, 3239.
- (6) For recent papers, see for example, (a) Duchateau, R.; van Santen, R. A.; Yap, G. P. A. *Organometallics* **2000**, *19*, 809. (b) Abbenhuis, H. C. L. *Chem. Eur. J.* **2000**, *6*, 25. (c) Mattori, M.; Mogi, K.; Sakai, Y.; Isobe, T. *J. Phys. Chem. A* **2000**, *104*, 10868. (d) Uzunova, E. L.; St. Nikolov, G. *J. Phys. Chem. B* **2000**, *104*, 7299. (e) Zhang, C.; Laine, R. M. *J. Am. Chem. Soc.* **2000**, *122*, 6979. (f) Kudo, T.; Gordon, M. S. *J. Phys. Chem. A* **2000**, *104*, 4058. (g) Skowronska-Ptasinska, M. D.; Duchateau, R.; van Santen, R. A.; Yap, G. P. A. *Organometallics* **2001**, *20*, 3519. (h) Lorenz, V.; Spoida, M.; Fischer, A.; Edelmann, F. T. *J. Organomet. Chem.* **2001**, *625*, 1. (i) Itoh, M. *KEISO KAGAKU KYOUKAISHI (J. Soc. Silicon Chem. Japan)* **2001**, *15*, 19. (j) Roggero, I.; Civalleri, B.; Ugliengo, P. *Chem. Phys. Lett.* **2001**, *341*, 625. (k) Kudo, T.; Gordon, M. S. *J. Phys. Chem. A* **2002**, *106*, 11347.
- (7) Kudo, T.; Gordon, M. S. *J. Phys. Chem. A* **2001**, *105*, 11276.
- (8) (a) Lee, C.; Yang, W.; Parr, R. G. *Phys. Rev.* **1988**, *B37*, 785. (b) Miehlich, B.; Savin, A.; Stoll, H.; Preuss, H. *Chem. Phys. Lett.* **1989**, *157*, 200. (c) Becke, A. D. *J. Phys. Chem.* **1993**, *98*, 5648.
- (9) (a) Hehre, W. J.; Ditchfield, R.; Pople, J. A. *J. Phys. Chem.* **1972**, *56*, 2257. (b) Francl, M. M.; Pietro, W. J.; Hehre, W. J.; Binkley, J. S.; Gordon, M. S.; Defrees, D. J.; Pople, J. A. *J. Chem. Phys.* **1982**, *77*, 3654. (c) Clark, T.; Chandrasekhar, J.; Spitznagel, G. W.; Schleyer, P. v. R. *J. Comput. Chem.* **1983**, *4*, 294. (d) Spitznagel, G. W.; Diplomarbeit, Erlangen, 1982. (e) Frisch, M. J.; Pople, J. A.; Binkley, J. S. *J. Chem. Phys.* **1984**, *80*, 3265. (f) Okuno, Y. J.; *Chem. Phys.* **1996**, *105*, 5817, and references therein.
- (10) Pople, J. A.; Seeger, R.; Krishnam, R. *Int. J. Quantum Chem.* **1979**, *S11*, 149.
- (11) Wachters, A. J. H. *J. Chem. Phys.* **1970**, *52*, 1033.
- (12) Schmidt, M. W.; Baldridge, K. K.; Boatz, J. A.; Elbert, S. T.; Gordon, M. S.; Jensen, J. H.; Koseki, S.; Matsunaga, N.; Nguyen, K. A.; Su, S.; Windus, T. L.; Dupuis, M.; Montgomery, J. A., Jr. *J. Comput. Chem.* **1993**, *14*, 1347.
- (13) Rappe, A. K.; Smedley, T. A.; Goddard, W. A. *J. Phys. Chem.* **1981**, *85*, 2607.
- (14) Frisch, M. J.; Trucks, G. W.; Schlegel, H. B.; Scuseria, G. E.; Robb, M. A.; Cheeseman, J. R.; Zakrzewski, V. G.; Montgomery, J. A.; Stratmann, R. E.; Burant, J. C.; Dapprich, S.; Millam, J. M.; Daniels, A. D.; Kudin, K. N.; Strain, M. C.; Farkas, O.; Toamsi, J.; Barone, G.; Cossi, M.; Cammi, R.; Mennucci, B.; Pomelli, C.; Adamo, C.; Clifford, S.; Ochterski, J.; Petersson, G. A.; Ayala, P. Y.; Cui, Q.; Morokuma, K.; Malick, D. K.; Rabuck, A. D.; Raghavachari, K.; Foresman, J. B.; Cioslowski, J.; Ortiz, J. V.; Stefanov, B. B.; Liu, G.; Lashenko, A.; Piskorz, P.; Komaromi, I.; Gomperts, R.; Martin, R. L.; Fox, D. J.; Keith, T.; Al-Laham, M. A.; Peng, C. Y.; Nanayakkara, A.; Gonzalez, C.; Challacombe, M.; Gill, P. M. W.; Johnson, B. G.; Chen, W.; Wong, M. W.; Andres, J. L.; Head-Gordon, M.; Replogle, E. S.; Pople, A. *Gaussian 98*; Gaussian, Inc.: Pittsburgh, PA, 1998.
- (15) Sharpless, K. B.; Woodward, S. S.; Finn, M. G. *Pure Appl. Chem.* **1983**, *55*, 1823.
- (16) (a) Maschmeyer, T.; Klunduk, M. C.; Martin, C. M.; Shephard, D. S.; Thomas, J. M.; Jonson, B. F. G. *Chem. Commun.* **1997**, 1847. (b) Pescarmona, P. P.; van der Waal, J.; Maxwell, I. E.; Maschmeyer, T. *Angew. Chem., Int. Ed.* **2001**, *40*, 740.
- (17) (a) Edelmann, F. T.; Giethmann, S.; Fischer, A. *J. Organomet. Chem.* **2001**, *620*, 80. (b) Lorenz, V.; Spoida, M.; Fischer, A.; Edelmann, F. T. *J. Organomet. Chem.* **2001**, *625*, 1.
- (18) Edelmann, F. T.; Giethmann, S.; Fischer, A. *Chem. Commun.* **2000**, 2153.
- (19) Cossee, P. *J. Catal.* **1964**, *80*.
- (20) Sakai, S. *J. Phys. Chem.* **1994**, *98*, 12053.